Nonlinear Dyn (2010) 61: 57–70
DOI 10.1007/s11071-009-9631-8

ORIGINAL PAPER

Differential quadrature method for analyzing nonlinear dynamic characteristics of viscoelastic plates with shear effects

J.-J. Li · C.-J. Cheng

Received: 8 June 2009 / Accepted: 20 November 2009 / Published online: 9 December 2009

Abstract The integro-partial differential equations governing the dynamic behavior of viscoelastic plates taking account of higher-order shear effects and finite deformations are presented. From the matrix formulas of differential quadrature, the special matrix product and the domain decoupled technique presented in this work, the nonlinear governing equations are converted into an explicit matrix form in the spatial domain. The dynamic behaviors of viscoelastic plates are numerically analyzed by introducing new variables in the time domain. The methods in nonlinear dynamics are synthetically applied to reveal plenty and complex dynamical phenomena of viscoelastic plates. The numerical convergence and comparison studies are carried out to validate the present solutions. At the same time, the influences of load and material parameters on dynamic behaviors are investigated. One can see that the system will enter into the chaotic state with a paroxysm form or quasi-periodic bifurcation with changing of parameters.

Keywords Viscoelastic plate · Finite deformation · Higher-order shear effect · Nonlinear dynamic analysis · Differential quadrature method

1 Introduction

Viscoelastic materials are widely applied in many fields of science and technology. The theory of viscoelasticity and its applications have become one of important branches in solid mechanics. But it is difficult to compute and analyze the nonlinear mechanical behavior of a viscoelastic structure due to the complexity of constitutive relation of material. There are papers for the analyses of dynamic behaviors of viscoelastic structures. Cederbaum et al. [1–3] used the phase diagram, Poincare section, power spectrum and the largest Lyapunov exponent to numerically study the chaos motion of viscoelastic plates. Cheng et al. [4–7] revealed the nonlinear dynamic properties of viscoelastic plates by using the Galerkin technique.

The differential quadrature method (DQM) is one kind of the high efficiency methods for solving complex boundary valued problems [8–23]. In order to expediently apply and to improve the efficiency and accuracy of the DQM, Wang and Bert [10, 11] presented an approach to deal with boundary conditions.

Sponsored by: the Major Research Plan of the National Natural Science Foundation of China (No. 90816001), the National Science Foundation for Post-doctoral Scientists of China (No. 20080440613); the Shanghai Postdoctoral Sustentation Fund, China (No. 09R21412700), the Shanghai Leading Academic Discipline Project (No. S30106).

J.-J. Li · C.-J. Cheng (✉)
Department of Mechanics, Shanghai Institute of Applied Mathematics and Mechanics, Shanghai University, Shanghai 200072, P.R. China
e-mail: chjcheng@mail.shu.edu.cn

J.-J. Li
e-mail: jjli@staff.shu.edu.cn

Chen [12, 13] introduced the special matrix product to express nonlinear a partial differential operator as an explicit matrix form. A method coupled with a geometrical transformation technique and domain decomposition method, is applied to solve two major limitations in application of the DQM [15–20]. Based on the first-order shear deformation theory (FSDT), Liew et al. [21] studied the bending and buckling of laminated plates by the moving least-squares DQM. Liew et al. [22, 23] applied a semi-analytical Galerkin-differential quadrature to analyze the post-buckling and the dynamic stability of FGM plates based on the higher-order shear deformation theory (HSDT). Li and Cheng [24] used the DQM to analyze the nonlinear vibration of orthotropic rectangular plates. More recently, based on FSDT, Malekzadeh et al. [25–28] analyzed the large deformation of thin composite plates and moderately thick composite plates by the DQM. Wang et al. [29] analyzed to the buckling of thin rectangular plates with the cosine-distributed compressive load on two opposite sides. But there is no report for the nonlinear analyses of viscoelastic plates taking account of both the higher-order shear effect and finite deformation by the DQM.

Based on the Reddy's theory of plates with the higher-order shear deformations and the Boltzmann superposition principle, a set of integro-partial differential equations governing the dynamic behaviors of viscoelastic plates with the geometric nonlinearity are firstly presented in the present paper. In order to solve the problem, the differential quadrature method is applied to discretize the governing equations on the spatial domain, and a set of integro-differential equations with regard to the time are yielded. A technique similar to the method in [12, 24] is further extended to realize the nonlinear computation. Then, the dynamic behaviors of viscoelastic plates are numerically computed and analyzed by introducing new variables on the time domain. The numerical convergence and comparison studies are carried out to validate the present solutions, and the influences of the load and material parameters on the nonlinear dynamic behaviors of viscoelastic plates are considered.

2 Mathematical formulation of the problem

Consider the transverse motion of a viscoelastic rectangular plate taking account of the transverse shear effect and finite deformation. Assume that a is the length, b the width and h the thickness, and that the plate is subjected to a transverse harmonic load $q(x, y, t)$. Let u, v and w be the displacements in the x, y, z directions, φ and ψ the mid-plane rotations about the x and y axes, respectively; then the spatial domain occupied by the rectangular plate may be expressed as $\Omega = \{(x, y) : 0 \le x \le a, 0 \le y \le b\}$.

For linear, isotropic, viscoelastic materials, the stress–strain relation may be given by the Boltzmann superposition principle, namely

$$\sigma_{ij} = C_1 \oplus \varepsilon_{ij} + \delta_{ij} C_2 \oplus \varepsilon_{kk} \quad (i, j = 1, 2, 3) \tag{1}$$

in which, $C_1 = L^{-1}[1/(s^2\overline{J}_1)]$, $C_2 = L^{-1}\{(\overline{J}_1 - \overline{J}_2)/[s^2\overline{J}_1(\overline{J}_1 + 2\overline{J}_2)]\}$, J_1 and J_2 are the creep functions of material, $\overline{(\cdot)}$ and L^{-1} express the Laplace transformation and its inverse transformation, s is a transformation parameter. The symbol $\oplus$ is the Boltzmann operator defined by

$$\begin{aligned}\psi_1(t) \oplus \psi_2(t) &= \psi_1(0)\psi_2(t) + \dot{\psi}_1(t) * \psi_2(t) \\ &= \psi_1(0)\psi_2(t) + \int_0^t \dot{\psi}_1(t-\tau)\psi_2(\tau)\,d\tau\end{aligned} \tag{2}$$

If Poisson ratio of material is independent of time, namely, $\mu(t) = \text{const}$, we get

$$J_2(t)/J_1(t) = (1 - 2\mu)/(1 + \mu),$$

$$C_2(t)/C_1(t) = \mu/(1 - \mu) = \mu_1$$

Following the Reddy's theory of plates [30] and ignoring the in-plane inertia, the Karman-type equations of viscoelastic plates with finite deformations can be written as

$$L_1(U) + L_2(V) + \overline{L}_1(W) - \eta^{-2}\ddot{U} = 0,$$

$$L_2(U) + L_3(V) + \overline{L_3}(W) - \eta^{-2}\ddot{V} = 0,$$

$$\begin{aligned}&L_4(W) + L_5(\Phi) + L_6(\Psi) + \overline{L}(W, U) \\ &\quad + \overline{L}(W, V) + \overline{L}(W, W) \\ &\quad + Q - \ddot{W} - e_1\eta^{-2}\frac{\partial^2\ddot{W}}{\partial X^2} - e_1\xi^{-2}\eta^2\frac{\partial^2\ddot{W}}{\partial Y^2} \\ &\quad - e_2\eta^{-1}\frac{\partial\ddot{\Phi}}{\partial X} - e_2\xi\eta^{-1}\frac{\partial\ddot{\Psi}}{\partial Y} = 0,\end{aligned}$$

$$\begin{aligned}&L_5(W) + e_5\eta^2 L_1(\Phi) + e_6\eta^4 c_1 \oplus \Phi + e_5\eta^2 L_2(\Psi) \\ &\quad - e_3\ddot{\Phi} - e_4\eta^{-1}\frac{\partial\ddot{W}}{\partial X} = 0,\end{aligned}$$

$$L_6(W) + e_5\eta^2 L_3(\Psi) + e_6\eta^4 c_1 \oplus \Psi + e_5\eta^2 L_2(\Phi) - e_3\ddot{\Psi} - e_4\xi\eta^{-1}\frac{\partial \ddot{W}}{\partial Y} = 0$$
$$(x, y, t) \in \Omega \times (0, t_0) \tag{3}$$

where, the dimensionless parameters and the variables have been introduced by

$$X = x/a, \quad Y = y/b, \quad U = u(x, y)/h,$$
$$V = v(x, y, t)/h, \quad W = w(x, y, t)/h,$$
$$\Phi = \varphi(x, y, t), \quad \Psi = \psi(x, y, t),$$
$$\xi = a/b, \quad \eta = a/h,$$
$$c_1(t) = C_1(t)/C_1(0), \quad c_2(t) = C_2(t)/C_1(0),$$
$$Q = \frac{qa^4}{(1+\mu)C_1(0)h^4}, \quad \tau = t/s_0, \quad \tau_0 = \frac{t_0}{s_0},$$
$$s_0 = (a^2/h)\sqrt{\frac{\rho}{(1+\mu)C_1(0)}}$$

in which, t is the time, ρ is the density. The coefficients e_i, the linear and nonlinear integro- differential operators L_i, $\overline{L}_i$ and $\overline{L}$ in (3) may be all found in Appendix A.

For convenience, we assume that the edge of plate is simply-supported. So the boundary conditions may be given as

$$U = V = W = \Psi = \frac{\partial \Phi}{\partial X} = \frac{\partial^2 W}{\partial X^2} = 0, \quad X = 0, 1$$
$$U = V = W = \Phi = \frac{\partial \Psi}{\partial Y} = \frac{\partial^2 W}{\partial Y^2} = 0, \quad Y = 0, 1$$
$$t \in (0, t_0) \tag{4}$$

It is pointed out that the original form of the boundary condition (4) is also an integro-differential type, and here it has been treated with the help of Titchmarsh theorem [4].

Let the initial conditions be

$$U|_{t=0} = U_0, \quad V|_{t=0} = V_0, \quad W|_{t=0} = W_0,$$
$$\Phi|_{t=0} = \Phi_0, \quad \Psi|_{t=0} = \Psi_0,$$
$$\dot{U}|_{t=0} = U_1, \quad \dot{V}|_{t=0} = V_1, \quad \dot{W}|_{t=0} = W_1,$$
$$\dot{\Phi}|_{t=0} = \Phi_1, \quad \dot{\Psi}|_{t=0} = \Psi_1 \quad (x, y) \in \Omega \tag{5}$$

Equations (3), the boundary conditions (4) and the initial conditions (5) form a mathematical model governing dynamic analyses of viscoelastic plates accounting the effect of transverse shear deformations and finite deformations. It can be seen that they are a set of nonlinear integro-partial differential equations. Obviously, it is difficult to obtain the analytical solution of the problem. Next, the differential quadrature method will be used to discretize the governing equations and boundary conditions of the problem on the spatial domain.

3 Solution methods

Assume that $N_x \times N_y$ grid points are collocated respectively along x- and y-axes on the two-dimensional domain Ω. From [24],the DQ formulation in matrix form for the partial derivative of a function $F(X, Y)$ (representing U, V and W) in two-dimensional domain may be given as

$$\frac{\partial \mathbf{F}}{\partial X} = \overline{\mathbf{A}}_x\mathbf{F}, \qquad \frac{\partial^2 \mathbf{F}}{\partial X^2} = \overline{\mathbf{B}}_x\mathbf{F},$$
$$\frac{\partial^3 \mathbf{F}}{\partial X^3} = \overline{\mathbf{C}}_x\mathbf{F}, \qquad \frac{\partial^4 \mathbf{F}}{\partial X^4} = \overline{\mathbf{D}}_x\mathbf{F},$$
$$\frac{\partial \mathbf{F}}{\partial Y} = \mathbf{F}\overline{\mathbf{A}}_y^T, \qquad \frac{\partial^2 \mathbf{F}}{\partial Y^2} = \mathbf{F}\overline{\mathbf{B}}_y^T,$$
$$\frac{\partial^3 \mathbf{F}}{\partial Y^3} = \mathbf{F}\overline{\mathbf{C}}_y^T, \qquad \frac{\partial^4 \mathbf{F}}{\partial Y^4} = \mathbf{F}\overline{\mathbf{D}}_y^T,$$
$$\frac{\partial^2 \mathbf{F}}{\partial X \partial Y} = \overline{\mathbf{A}}_x\mathbf{F}\overline{\mathbf{A}}_y^T, \qquad \frac{\partial^3 \mathbf{F}}{\partial X \partial Y^2} = \overline{\mathbf{A}}_x\mathbf{F}\overline{\mathbf{B}}_y^T,$$
$$\frac{\partial^3 \mathbf{F}}{\partial X^2 \partial Y} = \overline{\mathbf{B}}_x\mathbf{F}\overline{\mathbf{A}}_y^T, \qquad \frac{\partial^4 \mathbf{F}}{\partial X^2 \partial Y^2} = \overline{\mathbf{B}}_x\mathbf{F}\overline{\mathbf{B}}_y^T \tag{6}$$

The DQ formulations in matrix form for the partial derivative of functions $\Phi(X, Y)$ and $\Psi(X, Y)$ are similar, and we have

$$\frac{\partial \mathbf{\Phi}}{\partial Y} = \mathbf{\Phi}\overline{\mathbf{A}}_y^T, \qquad \frac{\partial^2 \mathbf{\Phi}}{\partial Y^2} = \mathbf{\Phi}\overline{\mathbf{B}}_y^T,$$
$$\frac{\partial^3 \mathbf{\Phi}}{\partial X \partial Y^2} = \overline{\overline{\mathbf{A}}}_x\mathbf{\Phi}\overline{\mathbf{B}}_y^T,$$
$$\frac{\partial \mathbf{\Phi}}{\partial X} = \overline{\overline{\mathbf{A}}}_x\mathbf{\Phi}, \qquad \frac{\partial^2 \mathbf{\Phi}}{\partial X^2} = \overline{\overline{\mathbf{B}}}_x\mathbf{\Phi}, \qquad \frac{\partial^3 \mathbf{\Phi}}{\partial X^3} = \overline{\overline{\mathbf{C}}}_x\mathbf{\Phi},$$
$$\frac{\partial^2 \mathbf{\Phi}}{\partial X \partial Y} = \overline{\overline{\mathbf{A}}}_x\mathbf{\Phi}\overline{\mathbf{A}}_y^T,$$

$$\frac{\partial \boldsymbol{\Psi}}{\partial X} = \overline{\mathbf{A}}_x \boldsymbol{\Psi}, \qquad \frac{\partial^2 \boldsymbol{\Psi}}{\partial X^2} = \overline{\mathbf{B}}_x \boldsymbol{\Psi},$$

$$\frac{\partial^3 \boldsymbol{\Psi}}{\partial X^2 \partial Y} = \overline{\mathbf{B}}_x \boldsymbol{\Psi} \overline{\overline{\mathbf{A}}}_y^T,$$

$$\frac{\partial \boldsymbol{\Psi}}{\partial Y} = \boldsymbol{\Psi} \overline{\overline{\mathbf{A}}}_y^T, \qquad \frac{\partial^2 \boldsymbol{\Psi}}{\partial Y^2} = \boldsymbol{\Psi} \overline{\overline{\mathbf{B}}}_y^T,$$

$$\frac{\partial^3 \boldsymbol{\Psi}}{\partial Y^3} = \boldsymbol{\Psi} \overline{\overline{\mathbf{C}}}_y^T, \qquad \frac{\partial^2 \boldsymbol{\Psi}}{\partial X \partial Y} = \overline{\mathbf{A}}_x \boldsymbol{\Psi} \overline{\overline{\mathbf{A}}}_y^T \tag{7}$$

where, the unknown variables $\mathbf{F}$, $\boldsymbol{\Phi}$ and $\boldsymbol{\Psi}$ in (6) and (7) are unknown matrixes with the $(N_x-2)\times(N_y-2)$ order. $\overline{\mathbf{A}}$, $\overline{\mathbf{B}}$, $\overline{\mathbf{C}}$, $\overline{\mathbf{D}}$ and $\overline{\overline{\mathbf{A}}}$, $\overline{\overline{\mathbf{B}}}$, $\overline{\overline{\mathbf{C}}}$ with the subscripts x and y stand for the DQ weighting coefficient and modified weighting coefficient matrices for the first- and the second-order partial derivatives with regard to x and y, respectively. The superscript T means the transpose of matrix.

Applying the DQ matrix formulas (6) and (7), (3) can be discretized at each grid point inside the two-dimensional domain Ω. Further using the Hadamard and Kronecker products of matrices [12, 13, 24], the coupled nonlinear formulas can be converted into the explicit matrix forms as follows:

$$\mathbf{H}_1 \oplus \overline{\mathbf{U}} + \mathbf{H}_2 \oplus \overline{\mathbf{V}} + c_1 \oplus \left[\left(\mathbf{H}_7 \overline{\mathbf{W}} \right) \circ \left(\widehat{\mathbf{H}}_1 \overline{\mathbf{W}} \right) + \left(\mathbf{H}_8 \overline{\mathbf{W}} \right) \circ \left(\widehat{\mathbf{H}}_2 \overline{\mathbf{W}} \right) \right] = 0, \tag{8a}$$

$$\mathbf{H}_2 \oplus \overline{\mathbf{U}} + \mathbf{H}_3 \oplus \overline{\mathbf{V}} + c_1 \oplus \left[\left(\mathbf{H}_8 \overline{\mathbf{W}} \right) \circ \left(\widehat{\mathbf{H}}_3 \overline{\mathbf{W}} \right) + \left(\mathbf{H}_7 \overline{\mathbf{W}} \right) \circ \left(\widehat{\mathbf{H}}_2 \overline{\mathbf{W}} \right) \right] = 0, \tag{8b}$$

$$\begin{aligned} &\mathbf{H}_4 \oplus \overline{\mathbf{W}} + \mathbf{H}_{15} \oplus \overline{\boldsymbol{\Phi}} + \mathbf{H}_{16} \oplus \overline{\boldsymbol{\Psi}} \\ &+ \left(\widehat{\mathbf{H}}_5 \overline{\mathbf{W}} \right) \circ \left\{ c_1 \oplus \left[\mathbf{H}_7 \overline{\mathbf{U}} + \frac{1}{2} \left(\mathbf{H}_7 \overline{\mathbf{W}} \right) \circ \left(\mathbf{H}_7 \overline{\mathbf{W}} \right) \right] \right\} \\ &\times \left(\widehat{\mathbf{H}}_6 \overline{\mathbf{W}} \right) \circ \left\{ c_1 \oplus \left[\mathbf{H}_8 \overline{\mathbf{V}} + \frac{1}{2} \left(\mathbf{H}_8 \overline{\mathbf{W}} \right) \circ \left(\mathbf{H}_8 \overline{\mathbf{W}} \right) \right] \right\} \\ &+ \frac{2\eta^2}{2\mu_1 + 1} \left(\widehat{\mathbf{H}}_2 \overline{\mathbf{W}} \right) \circ \left\{ c_1 \oplus \left[\mathbf{H}_8 \overline{\mathbf{U}} + \mathbf{H}_7 \overline{\mathbf{V}} \right. \right. \\ &\left. \left. + \left(\mathbf{H}_7 \overline{\mathbf{W}} \right) \circ \left(\mathbf{H}_8 \overline{\mathbf{W}} \right) \right] \right\} + \widehat{\mathbf{Q}} \\ &- \ddot{\mathbf{W}} - e_1 \eta^{-2} \overline{\mathbf{B}}_x \ddot{\overline{\mathbf{W}}} - e_1 \xi^{-2} \eta^2 \ddot{\overline{\mathbf{W}}} \overline{\mathbf{B}}_y^T \\ &- e_2 \eta^{-1} \overline{\overline{\mathbf{A}}}_x \ddot{\overline{\boldsymbol{\Phi}}} - e_2 \xi \eta^{-1} \overline{\boldsymbol{\Psi}} \overline{\overline{\mathbf{A}}}_y^T = 0, \end{aligned} \tag{8c}$$

$$\mathbf{H}_9 \oplus \overline{\mathbf{W}} + \mathbf{H}_{10} \oplus \overline{\boldsymbol{\Phi}} + \mathbf{H}_{11} \oplus \overline{\boldsymbol{\Psi}} - e_3 \eta^{-1} \ddot{\overline{\boldsymbol{\Phi}}} - e_4 \eta^{-2} \overline{\mathbf{A}}_x \ddot{\overline{\mathbf{W}}} = 0, \tag{8d}$$

$$\mathbf{H}_{12} \oplus \overline{\mathbf{W}} + \mathbf{H}_{13} \oplus \overline{\boldsymbol{\Phi}} + \mathbf{H}_{14} \oplus \overline{\boldsymbol{\Psi}} - e_3 \eta^{-1} \ddot{\overline{\boldsymbol{\Psi}}} - e_4 \eta^{-2} \xi \ddot{\overline{\mathbf{W}}} \overline{\mathbf{A}}_y^T = 0 \tag{8e}$$

in which, $\widehat{\mathbf{H}}_i = \mathbf{H}_i / c_1$, the expressions of $\mathbf{H}_i$ are listed in Appendix B, and $\overline{\mathbf{U}}$, $\overline{\mathbf{V}}$, $\overline{\mathbf{W}}$, $\overline{\boldsymbol{\Phi}}$ and $\overline{\boldsymbol{\Psi}}$ are vectors generated by stacking the rows of the corresponding $(N_x-2)\times(N_y-2)$ rectangular matrixes $\mathbf{U}$, $\mathbf{V}$, $\mathbf{W}$, $\boldsymbol{\Phi}$ and $\boldsymbol{\Psi}$ into one-column vectors. $\widehat{\mathbf{Q}}$ is the load column vector. The symbol $\circ$ expresses the Hadamard product of matrices defined as $\mathbf{A} \circ \mathbf{B} = [a_{ij} b_{ij}] \in \mathbf{C}^{N \times M}$, where, $\mathbf{A} = [a_{ij}]$ and $\mathbf{B} = [b_{ij}] \in \mathbf{C}^{N \times M}$, $\mathbf{C}^{N \times M}$ denotes the set of $N \times M$ real matrices.

It has to be explained that the boundary conditions (4) have been considered when the coefficients in (8) are calculated [13, 24]. Thus, it is not necessary to consider the boundary conditions (4) for solving (8).

From [24], the coupling equations (8a–8e) can be decoupled and $\overline{\mathbf{W}}$, $\overline{\boldsymbol{\Phi}}$, $\overline{\boldsymbol{\Psi}}$ are now the basic unknown vectors, so that the computation effort is significantly alleviated. In the temporal domain, the set of discretization equations (8) will be further reduced to a set of ordinary differential equations by introducing new variables.

For standard linear solid materials, the relaxation function $c_1 = c_1(t)$ satisfies the following conditions:

$$\begin{aligned} &c_1(t) = c_0 + c_1 \exp(-\alpha t), \quad c_1(0) = c_0 + c_1 = 1, \\ &\dot{c}_1(t-\tau) = -S_1(t) \cdot S_2(\tau) \\ &\quad = -[c_1 \exp(-\alpha t)] \cdot [\alpha \exp(\alpha \tau)] \end{aligned} \tag{9}$$

in which, c_1 is the material parameter and α is the reciprocal of the relaxation time.

Introduce the following new variables:

$$\mathbf{y_1}(t) = \{\boldsymbol{\delta}(t)\}, \quad \mathbf{y_2}(t) = \left\{\dot{\boldsymbol{\delta}}(t)\right\},$$

$$\mathbf{y_3}(t) = \int_0^t \dot{c}_1(t-\tau) \left\{\overline{\boldsymbol{\delta}}(\tau)\right\} \mathrm{d}\tau,$$

$$\mathbf{y_4}(t) = \int_0^t \dot{c}_1(t-\tau) \left\{\overline{\boldsymbol{\delta}}_1(\tau)\right\} \mathrm{d}\tau,$$

$$\mathbf{y_5}(t) = \int_0^t \dot{c}_1(t-\tau) \left\{\overline{\boldsymbol{\delta}}_2(\tau)\right\} \mathrm{d}\tau,$$

$$\mathbf{y_6}(t) = \int_0^t \dot{c}_1(t-\tau)\left\{\overline{\boldsymbol{\delta}}_3(\tau)\right\} \mathrm{d}\tau \tag{10}$$

where

$$\{\boldsymbol{\delta}(t)\} = \left\{\overline{\mathbf{W}}, \overline{\boldsymbol{\Phi}}, \overline{\boldsymbol{\Psi}}\right\}^T,$$

$$\boldsymbol{\delta_1} = \mathbf{H}_7\overline{\mathbf{U}} + \frac{1}{2}\left(\mathbf{H}_7\overline{\mathbf{W}}\right) \circ \left(\mathbf{H}_7\overline{\mathbf{W}}\right),$$

$$\boldsymbol{\delta_2} = \mathbf{H}_8\overline{\mathbf{V}} + \frac{1}{2}\left(\mathbf{H}_8\overline{\mathbf{W}}\right) \circ \left(\mathbf{H}_8\overline{\mathbf{W}}\right),$$

$$\boldsymbol{\delta_3} = \mathbf{H}_8\overline{\mathbf{U}} + \mathbf{H}_7\overline{\mathbf{V}} + \left(\mathbf{H}_7\overline{\mathbf{W}}\right) \circ \left(\mathbf{H}_8\overline{\mathbf{W}}\right)$$

Then the ordinary differential equations (8) may be derived, which read

$$\dot{\mathbf{Y}} = \mathbf{F}(\mathbf{Y}) \tag{11}$$

in which,

$$\mathbf{Y} = \left\{\mathbf{y_0}, \mathbf{y_1}, \ldots, \mathbf{y_6}\right\}^T, \quad \mathbf{F} = \left\{\mathbf{F_0}, \mathbf{F_1}, \ldots, \mathbf{F_{25}}\right\}^T,$$

$$\mathbf{F_0} = 1,$$

$$\mathbf{F_1} = \mathbf{y_2},$$

$$\begin{aligned}\mathbf{F_2} = \mathbf{N}^{-1}\Big\{&\mathbf{M}_0(\mathbf{y_1} + \mathbf{y_3}) + \left(\overline{\overline{\mathbf{H}}}_5\mathbf{y_1}\right) \circ \left[\left\{\overline{\boldsymbol{\delta}}_1\right\} + \mathbf{y_4}\right] \\ &+ \left(\overline{\overline{\mathbf{H}}}_6\mathbf{y_1}\right) \circ \left[\left\{\overline{\boldsymbol{\delta}}_2\right\} + \mathbf{y_5}\right] \\ &+ \frac{2\eta^2}{2\mu_1 + 1}\left(\overline{\overline{\mathbf{H}}}_2\mathbf{y_1}\right) \circ \left[\left\{\overline{\boldsymbol{\delta}}_3\right\} + \mathbf{y_6}\right] + \overline{\widehat{\mathbf{Q}}}_0\Big\},\end{aligned}$$

$$\mathbf{F_3} = -\alpha\left(c_1\mathbf{y_1} + \mathbf{y_3}\right),$$

$$\mathbf{F_4} = -\alpha\left(c_1\left\{\overline{\boldsymbol{\delta}}_1\right\} + \mathbf{y_4}\right),$$

$$\mathbf{F_5} = -\alpha\left(c_1\left\{\overline{\boldsymbol{\delta}}_2\right\} + \mathbf{y_5}\right),$$

$$\mathbf{F_6} = -\alpha\left(c_1\left\{\overline{\boldsymbol{\delta}}_3\right\} + \mathbf{y_6}\right)$$

where

$$\mathbf{M}_0 = \begin{bmatrix} \mathbf{H}_4 & \mathbf{H}_{15} & \mathbf{H}_{16} \\ \mathbf{H}_9 & \mathbf{H}_{10} & \mathbf{H}_{11} \\ \mathbf{H}_{12} & \mathbf{H}_{13} & \mathbf{H}_{14} \end{bmatrix}$$

$\overline{\overline{\mathbf{H}}}_i$, $\overline{\widehat{\mathbf{Q}}}_0$ and $\{\overline{\boldsymbol{\delta}}_i\}$ are matrixes with the $3(N_x-2)(N_y-2) \times 3(N_x-2)(N_y-2)$ order, the load column vector and the displacement column vector generated by respectively extending $\mathbf{H}_i$, $\widehat{\mathbf{Q}}$ and $\boldsymbol{\delta}_i$. $\mathbf{N}$ is the matrix of material parameters.

It is clear that, from (5), the initial values for the nonlinear system (11) are given as

$$\begin{aligned}&\left(\mathbf{y_1}(0), \mathbf{y_2}(0), \mathbf{y_3}(0), \mathbf{y_4}(0), \mathbf{y_5}(0), \mathbf{y_6}(0)\right)^T \\ &= \left(\overline{\mathbf{W}}_0, \overline{\boldsymbol{\Phi}}_0, \overline{\boldsymbol{\Psi}}_0, \dot{\overline{\mathbf{W}}}_0, \dot{\overline{\boldsymbol{\Phi}}}_0, \dot{\overline{\boldsymbol{\Psi}}}_0, \{\mathbf{0}\}, \{\mathbf{0}\}, \{\mathbf{0}\}\right)^T\end{aligned} \tag{12}$$

Thus the problem is farther reduced to solving the initial value problems (11) and (12) for a given the relaxation function (9).

The grid spacing pattern in this paper is given as follows [9]:

$$\begin{aligned}X_i &= \frac{1}{2}\left[1 - \cos\frac{(i-1)\pi}{N_x - 1}\right], \quad i = 1, 2, \ldots, N_x, \\ Y_i &= \frac{1}{2}\left[1 - \cos\frac{(i-1)\pi}{N_y - 1}\right], \quad i = 1, 2, \ldots, N_y\end{aligned} \tag{13}$$

in which, X_i and Y_i are the coordinates of grid points collocated respectively in the x- and y-directions on the solution field Ω.

4 Numerical results and discussions

Applying the Runge–Kutta–Fehlberg method to (11), the time history curve, phase-trajectory diagram and Poincare section can all be obtained by the numerical methods in nonlinear dynamics and by software of Matlab.

To examine the reliability and accuracy of the DQ solutions in the present paper, the numerical convergence and comparison studies are carried out firstly. To compare the present DQ solutions with the other solutions in existing literature, we consider the numerical results of viscoelastic thin plates ignoring the effect of the shear deformation. For the quasi-static response of viscoelastic thin plates subjected to the step loads $Q(x, y, t) = q_0 H(t)$, the DQ solutions of the center deflections W with different grid points are shown in

Table 1 The center deflections of viscoelastic thin plate for the step load ($c_1 = 0.5$, $\alpha = 0.06$, $q_0 = 0.09$) $\times 10^{-3}$

t	W (5 × 5)	W (7 × 7)	W (9 × 9)	W (11 × 11)	W (13 × 13)	Levy [4]
10	5.0813	5.1155	5.1153	5.1152	5.1152	5.1123
20	5.8561	5.8955	5.8953	5.8952	5.8952	5.8918
30	6.4301	6.4734	6.4731	6.4731	6.4731	6.4693
40	6.8554	6.9015	6.9012	6.9011	6.9011	6.8971
50	7.1704	7.2186	7.2183	7.2183	7.2183	7.2141
60	7.4038	7.4536	7.4533	7.4532	7.4532	7.4489
70	7.5766	7.6276	7.6273	7.6272	7.6271	7.6228
80	7.7047	7.7566	7.7562	7.7562	7.7562	7.7517
90	7.7996	7.8521	7.8518	7.8517	7.8517	7.8471
100	7.8699	7.9228	7.9225	7.9225	7.9224	7.9179

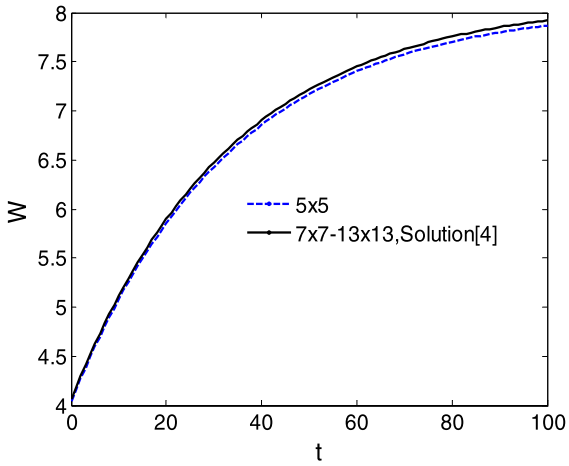

Fig. 1 Response for quasi-static motion

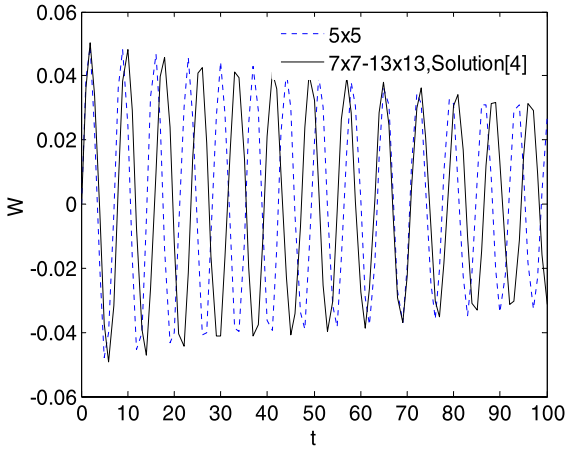

Fig. 2 Response for free vibrations

Table 1 and Fig. 1, respectively, together with the Levy analytical solutions W^* [4]. For the linear free vibrations of a viscoelastic square plate, the numerical solutions of the center deflections are obtained from the DQ method with respectively different grid points. Results are shown in Table 2 and Fig. 2, together with the other analytical solutions for the plate obtained by using Galerkin approach and Laplace transformation [4]. From Tables 1, 2 and Figs. 1, 2, one can see that the DQ solutions converge rapidly to the analytical results with the grid refinement. From Fig. 1 and Fig. 2, it can be also seen that the time history curves are obtained from the DQ solutions with 7 × 7 to 13 × 13 grid points, respectively, and they are the same as the analytical solutions [4]. Also, Table 1 and Fig. 1 show that it is sufficient to only employ 5 × 5 grid points and obtain very satisfactory results, with the relative error $(W^* - W_{5\times5})/W^* \leq 0.6\%$. At the same time, Fig. 2 and Table 2 show that there is a small difference between the results of the vibration systems with the 5 × 5 and 7 × 7 grid points quantitatively, but the whole variation trends of the systems are qualitatively the same. Hence, the present method has good convergence and accuracy.

Next, letting $\lambda = 1$, $\mu = 0.23$, $c_1 = 0.5$, $Q = q_0 \sin(\omega t)$, we consider the influences of the load amplitude q_0 and the material parameter α on the dynamic behavior of the viscoelastic plate with shear effects under the case of periodic excitations.

When $q_0 = 1$, $\alpha = 2$, the dynamic figures of the center deflection of plate are shown in Fig. 3. Also,

Table 2 The center deflections of viscoelastic thin plate for free vibrations ($c_1 = 0.1$, $\alpha = 0.01$)($\times 10^{-2}$)

t	DQ 5×5	DQ 7×7	DQ 9×9	DQ 11×11	DQ 13×13	Solutions [4]
10	4.8300	2.4422	2.4472	2.4489	2.4442	2.4453
20	−1.2017	−4.0266	−4.0319	−4.0338	−4.0287	−4.0299
30	−4.1135	4.4283	4.4280	4.4279	4.4281	4.4281
40	2.1242	−3.6280	−3.6174	−3.6138	−3.6235	−3.6213
50	3.2299	1.9545	1.9332	1.9258	1.9456	1.9411
60	−2.7459	0.0946	0.1224	0.1319	0.1061	0.1120
70	−2.2649	−1.9348	−1.9611	−1.9701	−1.9457	−1.9512
80	3.0785	3.1177	3.1334	3.1389	3.1242	3.1275
90	1.3086	−3.3748	−3.3732	−3.3726	−3.3741	−3.3738
100	−3.1317	2.7336	2.7127	2.7055	2.7249	2.7205

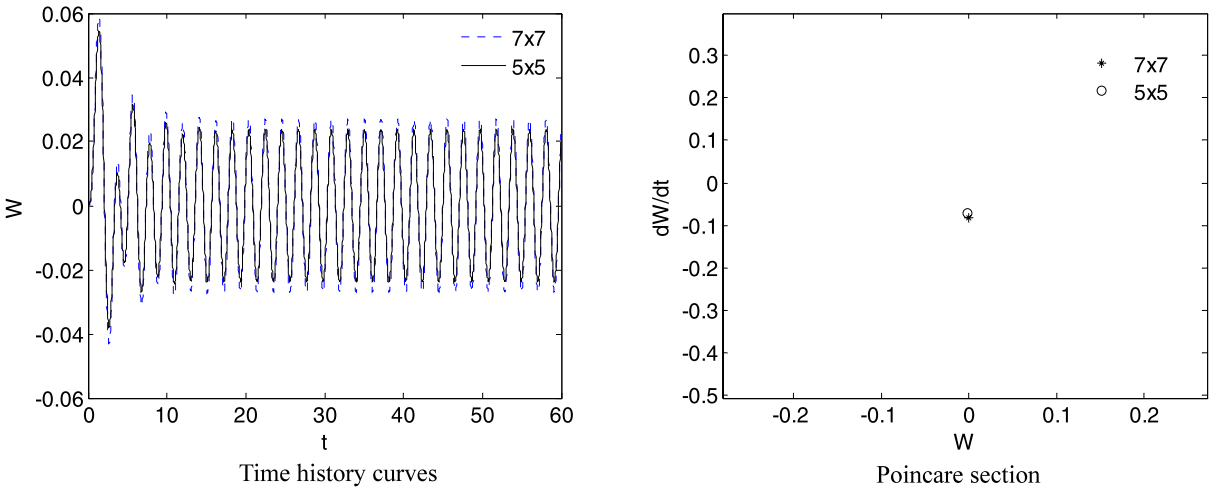

Fig. 3 Dynamic figures of the center deflection for different grid points

Fig. 3 shows the qualitative results obtained from the DQ solutions with the 5×5 and 7×7 grid points, and one can see that they are the same: the system has a stable period-1 attractor. Thus, in following computation, we will apply the 5×5 unequally grid points.

For given parameters, the dynamic figures of the center deflection are respectively shown in Figs. 4, 5, 6, 7.

When $\beta = 10$, the time history curves of the nonlinear free vibrations of plate for different α are shown in Fig. 4. It can be seen that attenuation velocity of nonlinear free vibrations is markedly increasing with increase of parameter α.

Figure 5 shows the phase-trajectory diagrams and the Poincare sections for different q_0 when $Q = q_0 \sin(\omega t)$, $\omega = 3$, $\beta = 10$. It is observed that with the increase of q_0 the system will translate from stability to un-stability and that will lead to chaotic motion for given material parameters α.

Figure 6 shows the phase-trajectory diagrams and the Poincare sections for different α when $Q = q_0 \sin(\omega t)$, $\omega = 3$, $\beta = 10$. From Fig. 5(d) and Fig. 6, it can be seen that they correspond to periodic, quasi-periodic motions and unstable chaotic motions of plate. At the same time, it is observed that the motion states transfer into stable periodic motions from unstable chaotic or quasi-periodic motions with increase of parameter α. This indicates that the increase of α helps to stabilize the viscoelastic plates. The system

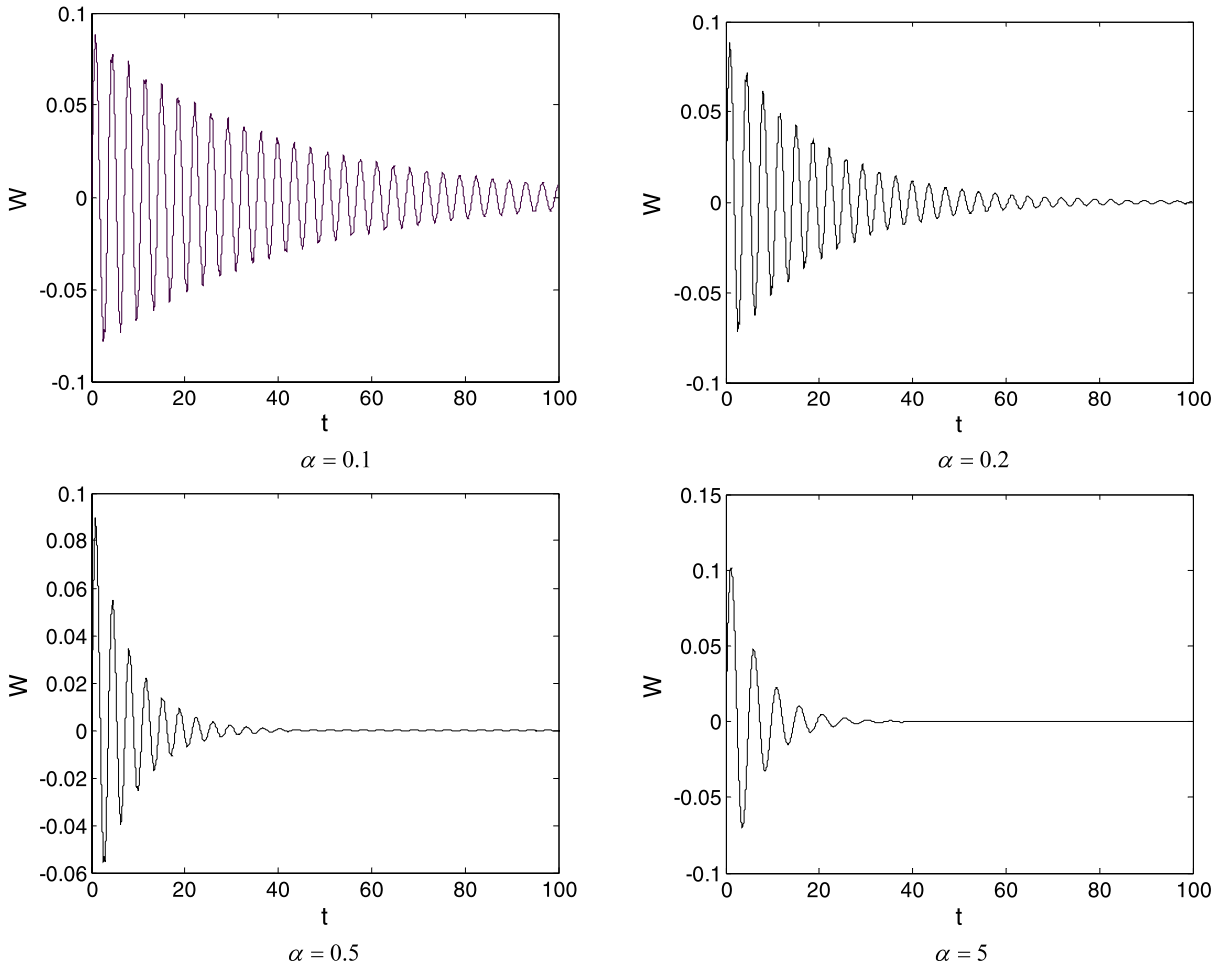

Fig. 4 Time history curves of the central deflection for $q_0 = 0$

will enter into the chaotic state with quasi-periodic bifurcation when the parameters change.

When $\alpha = 0$ or $c_1 = 0$, the system (12) degenerates into the nonlinear dynamic system of an elastic plate taking account of the transverse shear effect. The authors have not found reports on the dynamic analysis of elastic plates with the transverse shear deformation by DQM.

Figure 7 shows the phase-trajectory diagram and the Poincare section for different q_0 when the initial value $W_0 = 0$. It could be seen that the system translates from quasi-periodic motion to the chaotic motion when the load parameter q_0 increases. The corresponding Poincare section translates from a closed curve to infinitude points gathering out of a closed curve. Hence, the system also enters into the chaotic state with quasi-periodic bifurcation.

5 Conclusions

With the help of the differential quadrature method, the special matrix product and the domain decoupled technique in the spatial domain, as well as the introduction of new variables in the temporal domain, the dynamic behaviors of viscoelastic plates taking account of higher-order shear effects and finite deformations are studied. The methods in nonlinear dynamics are synthetically applied to reveal plenty and complex dynamical phenomena of viscoelastic plates, such as fixed point, limit cycle, quasi-periodicity, chaos, and so on. The numerical convergence and comparison studies show that the presented differential quadrature method is reliable and valid even when only a small grid scale is adopted. Furthermore, it can be seen that with the change of parameters the system enters into

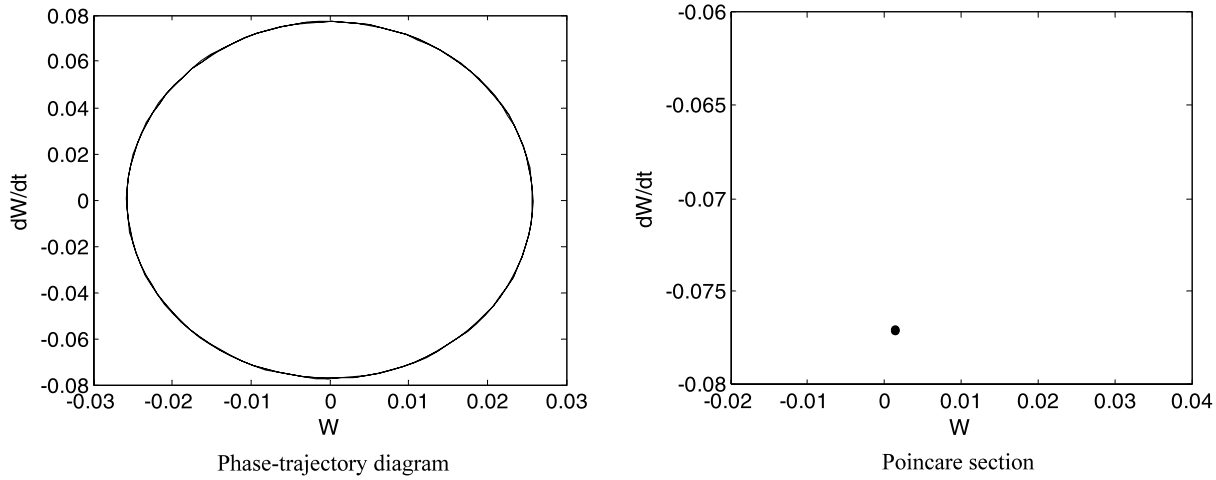

(a) $q_0 = 1$

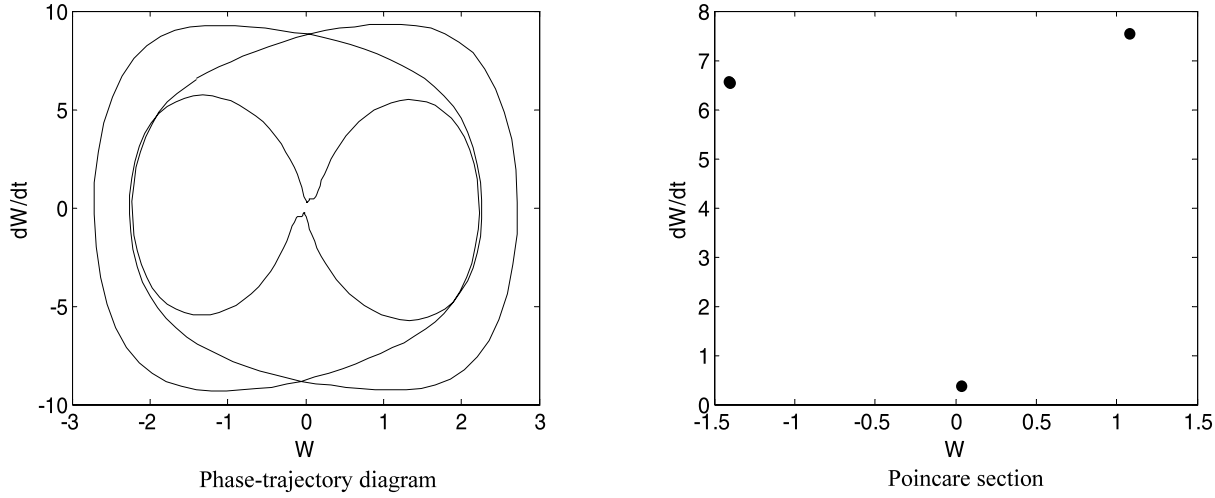

(b) $q_0 = 120$

Fig. 5 Dynamic figures of the center deflection for $\alpha = 0.1$

chaotic state with a paroxysm form or quasi-periodic bifurcation.

Appendix A

The coefficients e_i, operators $L_i(\bullet)$, $\overline{L}_i(\bullet)$ and $\overline{L}(\bullet)$ in (3) are defined by

$$e_1 = -1/252, \quad e_3 = 17/315, \quad e_2 = -e_4 = 4/315,$$
$$e_5 = -17/315, \quad e_6 = 4/15$$

$$L_1(\bullet) = (1+\mu_1)c_1 \oplus \frac{\partial^2}{\partial X^2} + \frac{\xi^2}{2}c_1 \oplus \frac{\partial^2}{\partial Y^2},$$

$$L_2(\bullet) = \left(\frac{1}{2}+\mu_1\right)\xi c_1 \oplus \frac{\partial^2}{\partial X \partial Y},$$

$$L_3(\bullet) = \frac{1}{2}c_1 \oplus \frac{\partial^2}{\partial X^2} + (1+\mu_1)\xi^2 c_1 \oplus \frac{\partial^2}{\partial Y^2},$$

$$\begin{aligned} L_4(\bullet) &= \left(\frac{1}{2}+\mu_1\right)\xi c_1 \oplus \frac{\partial^2}{\partial X \partial Y} \\ &= -\frac{1}{252}(1+\mu_1)c_1 \oplus \left(\frac{\partial^4}{\partial X^4} + \xi^4 \frac{\partial^4}{\partial Y^4} \right. \\ &\quad \left. + 2\xi^2 \frac{\partial^4}{\partial X^2 \partial Y^2}\right) \\ &\quad - \frac{4}{15}\eta^2 c_1 \oplus \left(\frac{\partial^2}{\partial X^2} + \xi^2 \frac{\partial^2}{\partial Y^2}\right), \end{aligned}$$

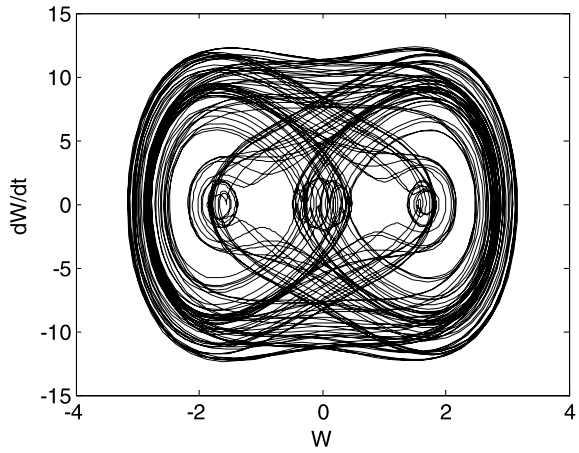

Phase-trajectory diagram

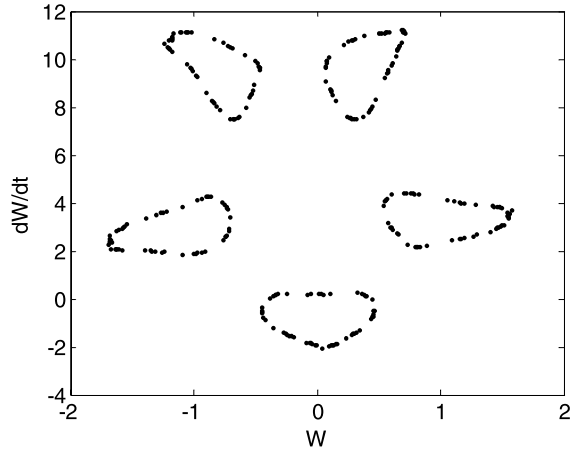

Poincare section

(c) $q_0 = 200$

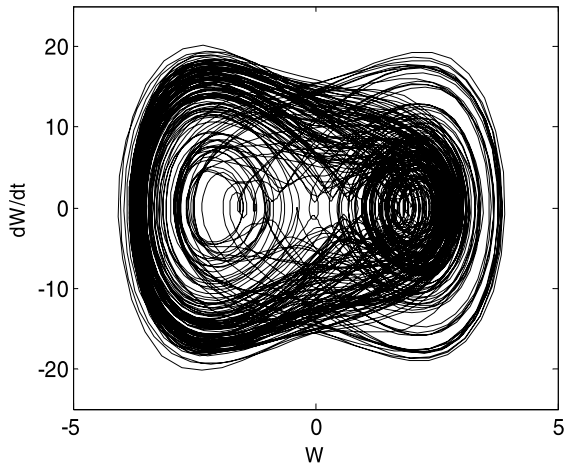

Phase-trajectory diagram

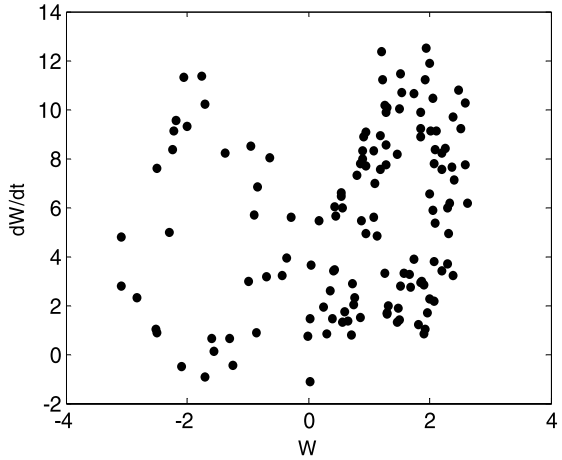

Poincare section

(d) $q_0 = 400$

Fig. 5 (*Continued*)

$$L_5(\bullet) = \left(\frac{1}{2} + \mu_1\right)\xi c_1 \oplus \frac{\partial^2}{\partial X \partial Y}$$
$$= \frac{4}{315}(1+\mu_1)\eta c_1 \oplus \left(\frac{\partial^3}{\partial X^3} + \xi^2 \frac{\partial^3}{\partial X \partial Y^2}\right)$$
$$- \frac{4}{15}\eta^2 c_1 \oplus \frac{\partial}{\partial X},$$

$$L_6(\bullet) = \frac{4}{315}(1+\mu_1)\eta\xi c_1 \oplus \left(\xi^2 \frac{\partial^3}{\partial Y^3} + \frac{\partial^3}{\partial X^2 \partial Y}\right)$$
$$- \frac{4}{15}\xi\eta^2 c_1 \oplus \frac{\partial}{\partial Y},$$

$$\overline{L}_1(\bullet) = \eta^{-1} L_1(\bullet)\frac{\partial}{\partial X}$$
$$+ \left(\frac{1}{2} + \mu_1\right)\eta^{-1}\xi^2 c_1 \oplus \left(\frac{\partial^2}{\partial X \partial Y}\frac{\partial}{\partial Y}\right),$$

$$\overline{L}_3(\bullet) = \xi\eta^{-1} L_3(\bullet)\frac{\partial}{\partial Y}$$
$$+ \left(\frac{1}{2} + \mu_1\right)\xi\eta^{-1} c_1 \oplus \left(\frac{\partial^2}{\partial X \partial Y}\frac{\partial}{\partial X}\right),$$

$$\overline{L}(W, U) = \eta\left[(1+\mu_1)\frac{\partial^2 W}{\partial X^2} + \xi^2\mu_1\frac{\partial^2 W}{\partial Y^2}\right]c_1 \oplus \frac{\partial U}{\partial X}$$
$$+ \eta\xi^2\frac{\partial^2 W}{\partial X \partial Y}c_1 \oplus \frac{\partial U}{\partial Y},$$

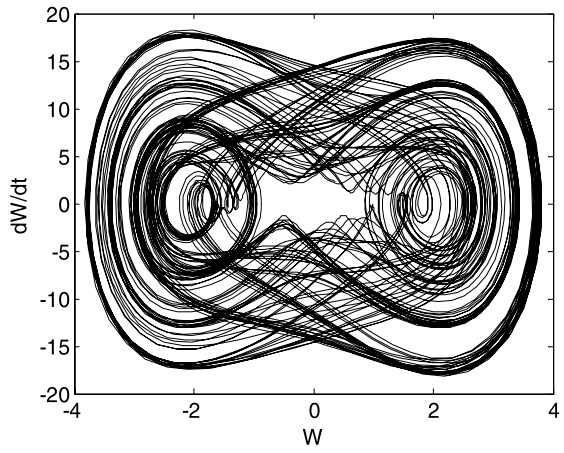

Phase-trajectory diagram

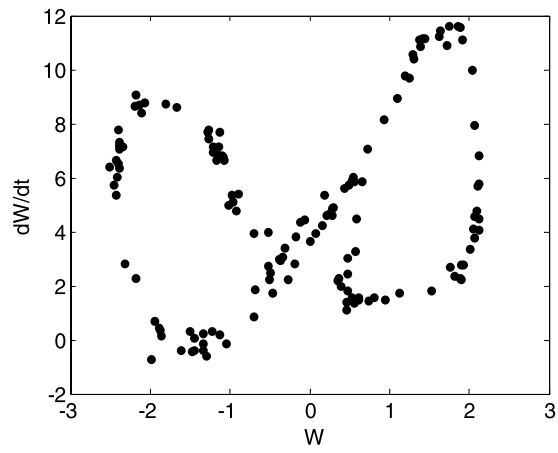

Poincare section

(a) $\alpha = 1$

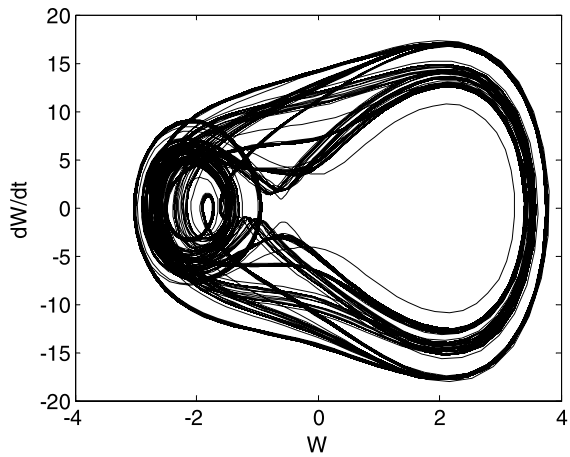

Phase-trajectory diagram

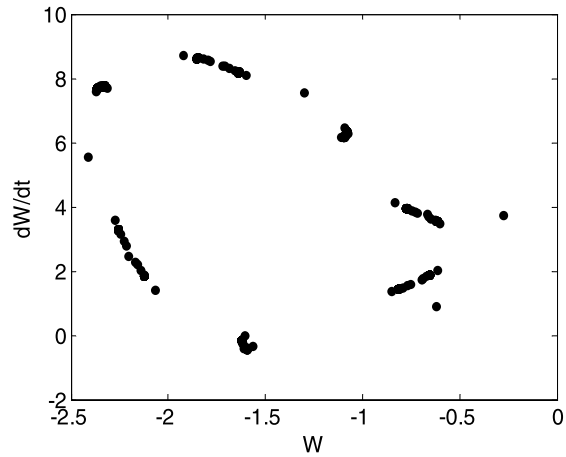

Poincare section

(b) $\alpha = 1.2$

Fig. 6 Dynamic figures of the central deflection for $q_0 = 400$

$$\overline{L}(W,V) = \eta\xi\left[\mu_1\frac{\partial^2 W}{\partial X^2} + \xi^2(1+\mu_1)\frac{\partial^2 W}{\partial Y^2}\right]c_1 \oplus \frac{\partial V}{\partial Y} + \eta\xi\frac{\partial^2 W}{\partial X\partial Y}c_1 \oplus \frac{\partial V}{\partial X},$$

$$\overline{L}(W,W) = \frac{1}{2}\left[(1+\mu_1)\frac{\partial^2 W}{\partial X^2} + \xi^2\mu_1\frac{\partial^2 W}{\partial Y^2}\right]c_1 \oplus \left(\frac{\partial W}{\partial X}\right)^2 + \frac{\xi^2}{2}\left[\mu_1\frac{\partial^2 W}{\partial X^2} + \xi^2(1+\mu_1)\frac{\partial^2 W}{\partial Y^2}\right]c_1 \oplus \left(\frac{\partial W}{\partial Y}\right)^2 + \xi^2\frac{\partial^2 W}{\partial X\partial Y}c_1 \oplus \left(\frac{\partial W}{\partial X}\frac{\partial W}{\partial Y}\right)$$

Appendix B

$\mathbf{H}_i$ in (9) are given as

$$\mathbf{H}_1 = a_1\left(\mathbf{I}_y \otimes \overline{\mathbf{B}}_x\right) + a_4\xi^2\left(\overline{\mathbf{B}}_y \otimes \mathbf{I}_x\right),$$

$$\mathbf{H}_2 = (a_3 + a_4)\xi\left(\overline{\mathbf{A}}_y \otimes \overline{\mathbf{A}}_x\right),$$

$$\mathbf{H}_3 = a_2\xi^2\left(\overline{\mathbf{B}}_y \otimes \mathbf{I}_x\right) + a_4\left(\mathbf{I}_y \otimes \overline{\mathbf{B}}_x\right),$$

$$\mathbf{H}_4 = g_1\left(\mathbf{I}_y \otimes \overline{\mathbf{D}}_x\right) + g_2\xi^4\left(\overline{\mathbf{D}}_y \otimes \mathbf{I}_x\right) + g_3\xi^2\left(\overline{\mathbf{B}}_y \otimes \overline{\mathbf{B}}_x\right) - g_7\eta^2\left(\mathbf{I}_y \otimes \overline{\mathbf{B}}_x\right) - g_8\xi^2\eta^2\left(\overline{\mathbf{B}}_y \otimes \mathbf{I}_x\right),$$

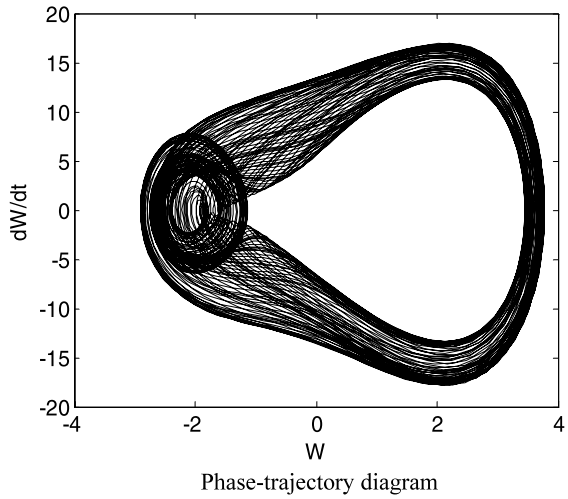

Phase-trajectory diagram

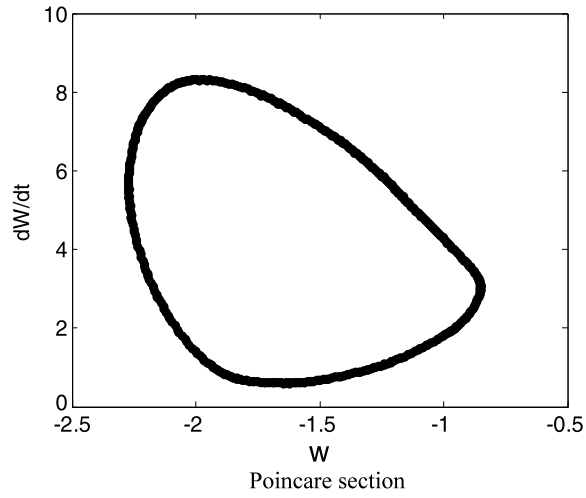

Poincare section

(c) $\alpha = 1.5$

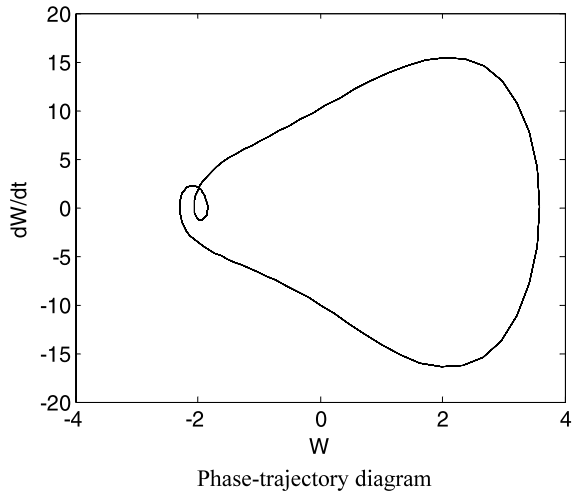

Phase-trajectory diagram

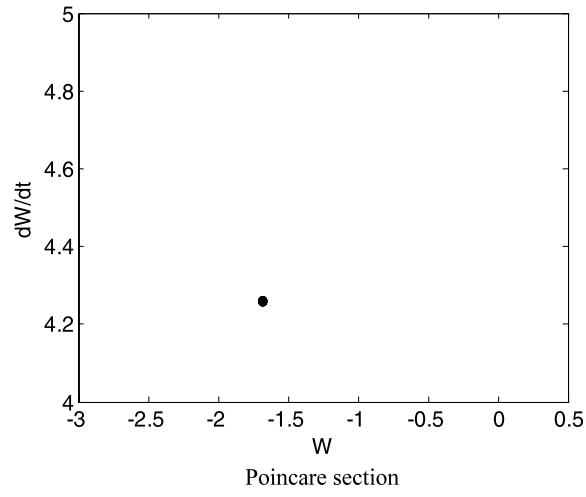

Poincare section

(d) $\alpha = 2$

Fig. 6 (*Continued*)

$$\mathbf{H}_5 = \xi^2\eta^2 a_3\big(\overline{\mathbf{B}}_y \otimes \mathbf{I}_x\big) + \eta^2 a_1\big(\mathbf{I}_y \otimes \overline{\mathbf{B}}_x\big),$$

$$\mathbf{H}_6 = \xi^2\eta^2 a_2\big(\overline{\mathbf{B}}_y \otimes \mathbf{I}_x\big) + \eta^2 a_3\big(\mathbf{I}_y \otimes \overline{\mathbf{B}}_x\big),$$

$$\mathbf{H}_7 = \eta^{-1}\big(\mathbf{I}_y \otimes \overline{\mathbf{A}}_x\big), \quad \mathbf{H}_8 = \xi\eta^{-1}\big(\overline{\mathbf{A}}_y \otimes \mathbf{I}_x\big),$$

$$\mathbf{H}_9 = -g_4\big(\mathbf{I}_y \otimes \overline{\mathbf{C}}_x\big) - g_6\xi^2\big(\overline{\mathbf{B}}_y \otimes \overline{\mathbf{A}}_x\big) + g_7\eta^2\big(\mathbf{I}_y \otimes \overline{\mathbf{A}}_x\big),$$

$$\mathbf{H}_{10} = g_{10}\eta\big(\mathbf{I}_y \otimes \overline{\overline{\mathbf{B}}}_x\big) + g_{11}\mu\xi\big(\overline{\mathbf{B}}_y \otimes \mathbf{I}_x\big) + g_7\eta^3(\mathbf{I}_y \otimes \mathbf{I}_x),$$

$$\mathbf{H}_{11} = g_9\eta\xi\big(\overline{\overline{\mathbf{A}}}_y \otimes \overline{\mathbf{A}}_x\big), \quad \mathbf{H}_{12} = g_9\eta\xi\big(\overline{\mathbf{A}}_y \otimes \overline{\overline{\mathbf{A}}}_x\big),$$

$$\mathbf{H}_{13} = -g_5\xi^3\big(\overline{\mathbf{C}}_y \otimes \mathbf{I}_x\big) - g_6\xi\big(\overline{\mathbf{A}}_y \otimes \overline{\mathbf{B}}_x\big) + g_8\xi\eta^2\big(\overline{\mathbf{A}}_y \otimes \mathbf{I}_x\big),$$

$$\mathbf{H}_{14} = g_{12}\eta\xi^2\big(\overline{\overline{\mathbf{B}}}_y \otimes \mathbf{I}_x\big) + g_{11}\eta\big(\mathbf{I}_y \otimes \overline{\mathbf{B}}_x\big) + g_8\eta^3(\mathbf{I}_y \otimes \mathbf{I}_x),$$

$$\mathbf{H}_{15} = g_4\eta\big(\mathrm{I}_y \otimes \overline{\overline{\mathbf{C}}}_x\big) + g_6\eta\xi^2\big(\overline{\mathbf{B}}_y \otimes \overline{\overline{\mathbf{A}}}_x\big) - g_7\eta^3\big(\mathrm{I}_y \otimes \overline{\overline{\mathbf{A}}}_x\big),$$

$$\mathbf{H}_{16} = g_5\eta\xi^3\big(\overline{\overline{\mathbf{C}}}_y \otimes \mathrm{I}_x\big) + g_6\xi\eta\big(\overline{\overline{\mathbf{A}}}_y \otimes \overline{\mathbf{B}}_x\big) - g_8\xi\eta^3\big(\overline{\overline{\mathbf{A}}}_y \otimes \mathrm{I}_x\big)$$

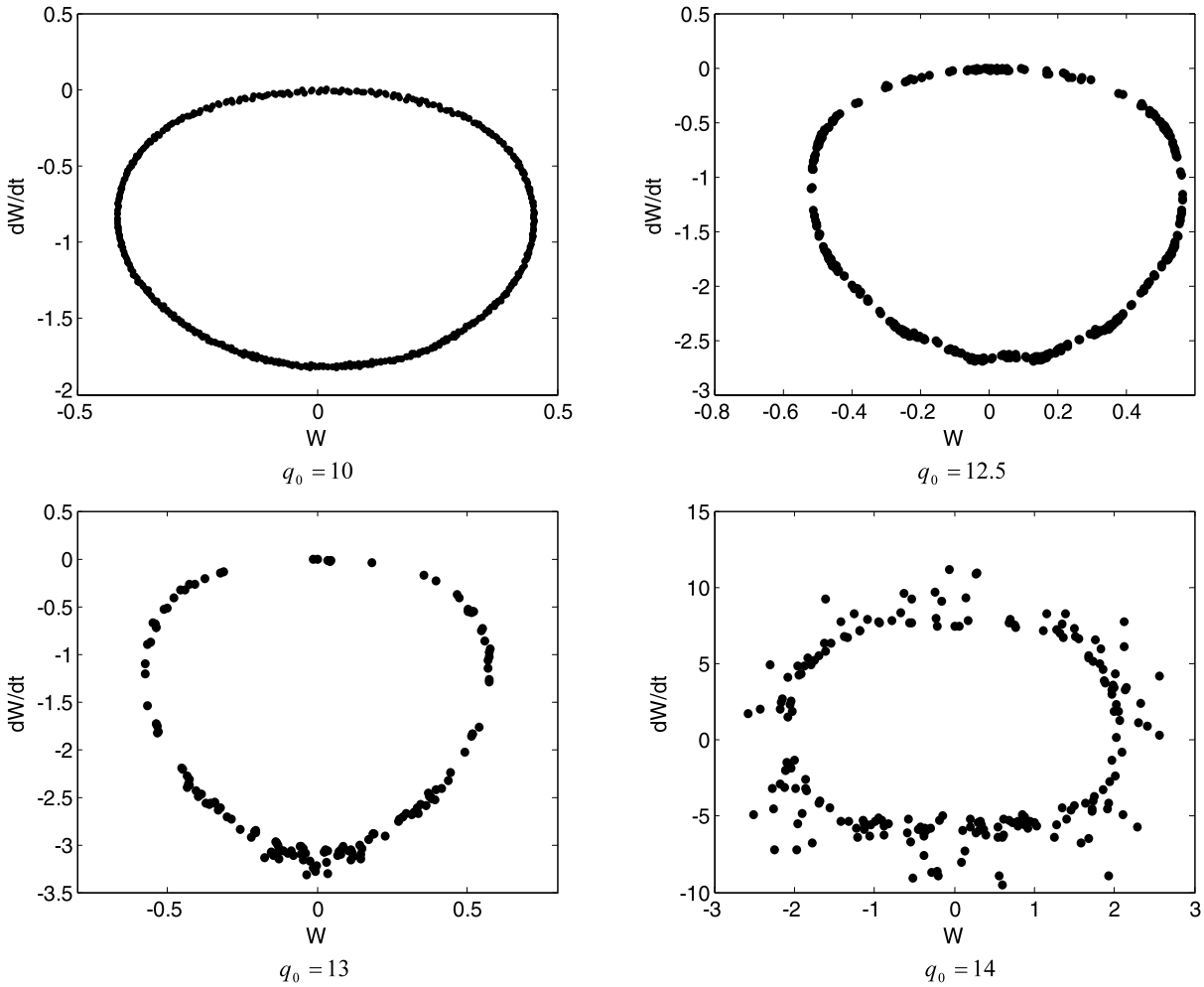

Fig. 7 Poincare sections of the central deflection for different q_0

in which, $\otimes$ expresses the Kronecker matrix product, $\mathbf{I}_x$ and $\mathbf{I}_y$ are the identity matrixes, a_i and g_i are given by

$$a_1 = a_2 = c_1 + c_2, \quad a_3 = c_2, \quad a_4 = c_1/2,$$

$$g_1 = g_2 = -(c_1 + c_2)/252, \quad g_3 = -(c_1 + c_2)/126,$$

$$g_4 = g_5 = 4(c_1 + c_2)/315, \quad g_6 = 4(c_1 + c_2)/315,$$

$$g_7 = g_8 = -4c_1/15, \quad g_9 = 17(c_1 + 2c_2)/630,$$

$$g_{10} = g_{12} = 17(c_1 + c_2)/315, \quad g_{11} = 17c_1/630$$

References

1. Cederbaum, G., Aboudi, J., Elishakoff, I.: Dynamic instability of shear-deformable viscoelastic laminated plates by Lyapunov exponents. Int. J. Solids Struct. **28**(3), 317–327 (1991)
2. Touati, D., Cederbaum, G.: Dynamic stability of nonlinear viscoelastic plates. Int. J. Solids Struct. **31**(17), 2367–2376 (1994)
3. Touati, D., Cederbaum, G.: Influence of large deflections on the dynamic stability of nonlinear viscoelastic plates. Acta Mech. **113**, 215–231 (1995)
4. Cheng, C.J., Zhang, N.H.: Variational principles on static-dynamic analysis of viscoelastic thin plates with applications. Int. J. Solids Struct. **35**(33), 4491–4505 (1998)
5. Zhang, N.H., Cheng, C.J.: Non-linear mathematical model of viscoelastic thin plates with its applications. Comput. Meth. Appl. Mech. Eng. **165**(4), 307–319 (1998)
6. Zhang, N.H., Cheng, C.J.: Two-mode Galerkin approach in dynamic stability. Appl. Math. Mech. **24**(3), 247–255 (2003)
7. Sheng, D.F., Cheng, C.J.: Dynamical behaviors of nonlinear viscoelastic thick plates with damage. Int. J. Solids Struct. **41**, 7287–7308 (2004)

8. Bert, C.W., Malik, M.: Differential quadrature method in computational mechanics: a review. Appl. Mech. Rev. **49**, 1–28 (1996)
9. Bert, C.W., Wang, X., Striz, A.G.: Differential quadrature for static and free vibrational analyses of anisotropic plates. Int. J. Solids Struct. **30**, 1737–1744 (1993)
10. Wang, X., Bert, C.W.: A new approach in applying differential quadrature to static and free vibrational analyses of beams and plates. J. Sound Vib. **162**, 566–572 (1993)
11. Want, X., Bert, C.W.: Differential quadrature analysis of deflection, buckling and free vibrations of beams and rectangular plates. Comput. Struct. **48**, 473–479 (1993)
12. Chen, W.: Differential quadrature method and its applications in engineering. Ph.D. dissertation, Shanghai Jiao Tong University, China (1996)
13. Chen, W., Shu, C., He, W., Zhong, T.: The applications of special matrix products to differential quadrature solution of geometrically nonlinear bending of orthotropic rectangular plates. Comput. Struct. **74**, 65–76 (2000)
14. Liew, K.M., Han, J.B., Xiao, Z.M.: Differential quadrature method for thick symmetric cross-ply laminates with first-order shear flexibility. Int. J. Solids Struct. **33**, 2647–2658 (1996)
15. Han, J.B., Liew, K.M.: An eight-node curvilinear differential quadrature formulation for Reissner/Mindlin plates. Comput. Meth. Appl. Mech. Eng. **141**, 265–280 (1997)
16. Liew, K.M., Teo, T.M., Han, J.B.: Comparative accuracy of DQ and HDQ methods for three-dimensional vibration analysis of rectangular plates. Int. J. Num. Meth. Eng. **45**, 1831–1848 (1999)
17. Teo, T.M., Liew, K.M.: Three-dimensional elasticity solutions to some orthotropic plate problems. Int. J. Solids Struct. **36**, 5301–5326 (1999)
18. Liu, F.L., Liew, K.M.: Analysis of vibrating thick rectangular plates with mixed boundary constraints using differential quadrature element method. J. Sound Vib. **225**(5), 915–934 (1999)
19. Liu, F.L., Liew, K.M.: Free vibration analysis of Mindlin sector plates: Numerical solutions by differential quadrature method. Comput. Meth. Appl. Mech. Eng. **177**, 77–92 (1999)
20. Liew, K.M., Teo, T.M., Han, J.B.: Three-dimensional static solutions of rectangular plates by variant differential quadrature method. Int. J. Mech. Sci. **43**, 1611–1628 (2001)
21. Liew, K.M., Huang, Y.Q.: Bending and buckling of thick symmetric rectangular laminates using the moving least-squares differential quadrature method. Int. J. Mech. Sci. **45**, 95–114 (2003)
22. Liew, K.M., Yang, J., Kitipornchai, S.: Postbuckling of the piezoelectric FGM plates subjected to thermo-electro-mechanical loading. Int. J. Solids Struct. **40**, 3869–3892 (2003)
23. Yang, J., Liew, K.M., Kitipornchai, S.: Dynamic stability of laminated FGM plates based on higher-order shear deformation theory. Comput. Mech. **33**, 305–315 (2004)
24. Li, J.J., Cheng, C.J.: Differential quadrature method for nonlinear vibration of orthotropic plates with finite deformations and transverse shear effect. J. Sound Vib. **281**, 295–309 (2005)
25. Malekzadeh, P., Karami, G.: Differential quadrature nonlinear analysis of skew composite plates based FSDT. Eng. Struct. **28**, 1307–1318 (2006)
26. Karami, G., Malekzadeh, P., Mohebpour, S.R.: DQM free vibration analysis of moderately thick symmetric laminated plates with elastically restrained edges. Compos. Struct. **74**, 115–125 (2006)
27. Malekzadeh, P., Sctoodch, A.R.: Large deformation analysis of moderately thick laminated plates on nonlinear elastic foundation by DQM. Compos. Struct. **80**, 569–579 (2007)
28. Malekzadeh, P.: A differential quadrature nonlinear free vibration analysis of laminated composite skew thin plates. Thin-Walled Struct. **45**, 237–250 (2007)
29. Wang, X., Gan, L., Zhang, Y.: Differential quadrature analysis of the buckling of thin rectangular plates with cosine-distributed compressive loads on two opposite sides. Adv. Eng. Softw. **39**, 497–504 (2008)
30. Reddy, J.N.: A refined nonlinear theory of plates with transverse shear deformation. Int. J. Solids Struct. **20**(9/10), 881–896 (1984)